Interpretation of the photoelectron spectra of superalkali species: Na_3O and Na_3O^-

Cite as: J. Chem. Phys. **136**, 224305 (2012); https://doi.org/10.1063/1.4728073
Submitted: 22 March 2012 . Accepted: 24 May 2012 . Published Online: 12 June 2012

S. Zein, and J. V. Ortiz

Interpretation of the photoelectron spectra of superalkali species: Na_3O and Na_3O^-

S. Zein and J. V. Ortiz[a)]
Department of Chemistry and Biochemistry, Auburn University, Auburn, Alabama 36349-5312, USA

(Received 22 March 2012; accepted 24 May 2012; published online 12 June 2012)

Recently measured photoelectron spectra of the Na_3O^- anion have been interpreted with the aid of *ab initio* electron propagator calculations. As in the case of the Li_3O^-, we propose that the photoionization of ground and excited neutral states, in a sequential two photon absorption mechanism, plays a role in the interpretation of the observed spectrum. The lowest vertical electron detachment energy of Na_3O^- corresponds to a Dyson orbital that is composed chiefly of diffuse Na s functions and connects a D_{3h} singlet anion to an uncharged species with the same point group. Electron binding energies of isomers of the anion with different point groups or multiplicities have been considered. The relative magnitudes of the ionization energies of the neutral Li_3O and Na_3O species are also discussed. Whereas the most recent experimental data hold that Na_3O has the higher ionization energy, this work asserts the opposite trend. © *2012 American Institute of Physics*. [http://dx.doi.org/10.1063/1.4728073]

INTRODUCTION

Discovery of novel ionic solids and other unusual materials motivates the search for highly electropositive molecules or ions with low ionization energies (IEs) or electron detachment energies.[1–3] The IEs of superalkali molecules and the electron detachment energies of superalkali anions are smaller than their atomic, alkali counterparts. Hypermetalated molecules with the general formula XM_n consist of a relatively electronegative main group element (X = O, N, C, ...) surrounded by a shell of metal atoms (M = Li, Na, K...). They exhibit an exceptional stability and a potential violation of the octet rule. These species are characterized by highest occupied molecular orbitals that have bonding character among metallic atoms and X-M antibonding character. Hypermetalated molecules are also excellent candidates for superatoms.

Several experimental,[4,5] theoretical,[1–3,6–8] and combined[9] studies have been devoted to the investigation of superalkalis. The focus of these studies has been exclusively on neutral and cationic species. Much attention was attracted to these systems by the pioneering computational efforts of the Boldyrev group in 1982[2] where the IE of the Na_3O was estimated to be 3.48 eV from variational discrete X_α calculations performed with the double -ζ basis set of Clementi.[10] The first experiments on this system were performed subsequently via photoionization measurements of the appearance potentials of mass-determined, oxidized metal clusters formed by reactions in a molecular beam.[4] The extracted value of the IE through logarithmic plots (Watanabe plots after the method of Berkowitz[11]) was found to be 3.9 ± 0.15 eV. Wuerthwein and Schleyer recalculated the ground state of Na_3O and found, at the HF/6-31G* level of theory, an IE of 2.92 eV.[12] A higher level of theory,[13] MP2/6-31+G*, later yielded 3.22 eV. This study included six computational methods (PMP2, PMP3, PMP4, QCISD, QCISD(T), QCISD(T)+ZPE) and three basis sets (6-31+G*, 6-311+G*, and 6-311+G(2df)) that led to 24 values of the IE confined to the 3.1–3.4 eV energy range. Zakrzewski *et al.*[6] undertook the first electron propagator calculations on the system, evaluating an IE of 3.13 eV from the Outer Valence Green's Function (OVGF) method. On the other hand, the measured value was lowered to 3.53 eV by a newer study of Vituccio *et al.*[5] using photoionization efficiency techniques. To our knowledge, the latest re-measurement of the Na_3O IE was made using photodepletion spectroscopy coupled with one-photon ionization mass spectroscopy[9] and produced a value of 3.69 ± 0.15 eV. Theoretical work accompanying this same experimental study was performed using a variety of basis sets. The best calculated value according to these authors was 3.34 eV.[9] Elliott and Ahlrichs[8] carried out B3LYP and MP2 calculations, getting 3.68 and 3.24 eV, respectively. Finally, the most recent theoretical study on the subject found an IE of 3.76 eV using a density functional method with a double-ζ plus polarization basis set.[3]

We recently considered the detailed study of geometrical and electronic structures of the Li_3O^- and Li_3O species and refer the reader to it for a better comprehension of the present text.[14] Bearing in mind the basic concepts explaining the lowering of the IE of alkali atoms when going down the periodic table, we find that the current relative trend of the hypermetallic lithium and sodium compounds is counterintuitive, at least on the basis of experimental data. The latest study shows that the IE of Li_3O is 3.45 eV, that is, *smaller* than the value of 3.69 eV found for Na_3O.[9] This value for Li_3O was measured in 1979 to be 4.52 ± 0.2 eV[15] and later to be 3.54 ± 0.3 eV.[16] Notice here that at the beginning of the 1980s, the trend was still as expected, but the progression in the measurements (that changed dramatically by over 1 eV) may imply the opposite trend.

a)ortiz@auburn.edu.

This paper considers the interpretation of the latest photoelectron spectra of the Na_3O^- and Na_3O species.[17] We will examine first the relative stabilities of several, possible nuclear configurations of the Na_3O^- anion in singlet and triplet states. Vertical electron detachment energies and ionization energies of the anionic and neutral species will be evaluated using electron propagator techniques. The relative IEs of the neutral M_3O species with M = Li or Na will also be discussed. It will be shown that neither the anionic, nor the neutral photoelectron spectrum is sufficient for the attribution of all observed peaks in the experimental spectra. Thus, this paper supports a sequential two photon absorption mechanism, as in the M = Li case.

THEORY

In electron propagator theory, the Dyson equation provides the foundation of practical calculations and subsequent, qualitative interpretation. The solutions of the Dyson equation may take the following form:

$$[\mathbf{F} + \mathbf{\Sigma}(\varepsilon_i)]\Phi_i = \varepsilon_i \Phi_i, \tag{1}$$

where $\mathbf{F}$ and $\mathbf{\Sigma}$ are the Fock and self-energy operator matrices, respectively. Φ is a Dyson orbital that is defined as the overlap between the N and N-1 many-electron wave functions according to

$$\Phi(1) = \sqrt{N} \int \Psi_I^N(1, \ldots, N)\Psi_F^{N-1}(2, \ldots, N)d2, \ldots dN. \tag{2}$$

I and F stand for initial and final states. Φ can be built from the canonical Hartree-Fock molecular orbitals, as in the case of the P3[18] method, or from Brueckner orbitals as in the BD-T1[19,20] case. Dyson orbitals can be used for the calculations of electron momentum spectra[21,22] and interpretation of other orbital imaging experiments.[23–25]

In general, the Dyson orbitals are not normalized to unity. Their norms represent the pole strengths (PS) and may vary between zero and one, such that

$$\mathrm{PS} = \int |\Phi(1)|^2 \, d1. \tag{3}$$

Photoionization intensities, transition probabilities, and electron scattering cross sections are proportional to the pole strengths. Another formula for the PS can be seen, according to the quasiparticle (or diagonal self-energy) approach,[26] in the following expression:

$$\mathrm{PS} = \left. \frac{1}{1 - \dfrac{d\mathbf{\Sigma}(E)}{dE}} \right|_{E=\varepsilon}, \tag{4}$$

where the dependence of the PS on the variation of the diagonal elements of the self-energy matrix is shown.

COMPUTATIONAL DETAILS

Quantum chemical calculations and illustrations of molecular frames (Figs. 1 and 2) and orbitals (Figs. 3 and 4) were produced with the GAUSSIAN 03 (Ref. 27) code and its GaussView extension. Numerical coupled-cluster singles and doubles plus perturbative triples (CCSD(T))[28,29] geometry optimizations and harmonic frequency calculations were done with the 6-311+G*[30,31] basis set. Vertical electron detachment energies (VEDEs) and IEs were estimated using electron propagator theory (EPT) methods. Closed-shell electronic configurations were characterized with the BD-T1 (Refs. 19 and 20) approximation and the P3 (Ref. 18) approximation was used for triplet initial states. The IEs of the neutral species were evaluated as electron affinities (EAs) of the closed-shell cation. Two basis sets were used for the EPT calculations: 6-311+G* and 6-311+G(2df) plus two series of diffuse s, p, d, f functions on Na and O atoms. The coefficients of the diffuse functions were obtained by dividing the smallest coefficients for each atomic orbital in the 6-311+G(2df) basis by four. Only 1*s*-like molecular orbitals on oxygen and sodium are omitted from consideration in the correlated calculations.

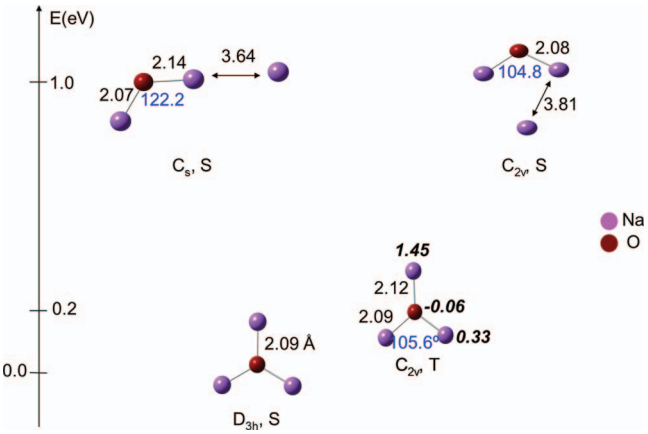

FIG. 1. Molecular structures and bond lengths of the stationary points on the Na_3O potential energy surface. Spin density distribution is given in *bold italic* when nonzero. S and T refer to singlets and triplets, respectively.

RESULTS AND DISCUSSION

Molecular structures

The chief structural precedent that can be found in the literature of Na_3O and its ions has one oxygen atom sur-

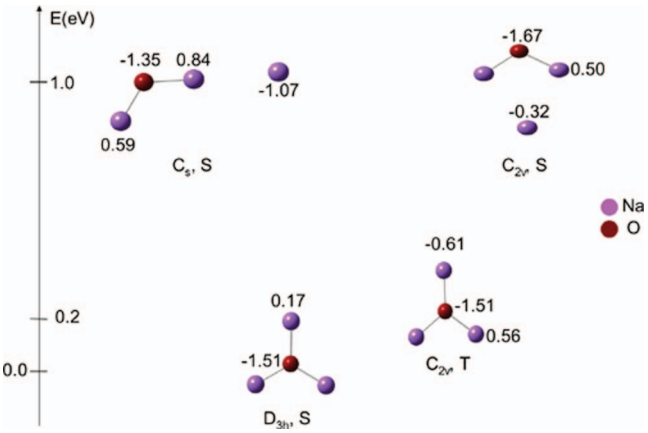

FIG. 2. Mulliken charge distributions of local minima.

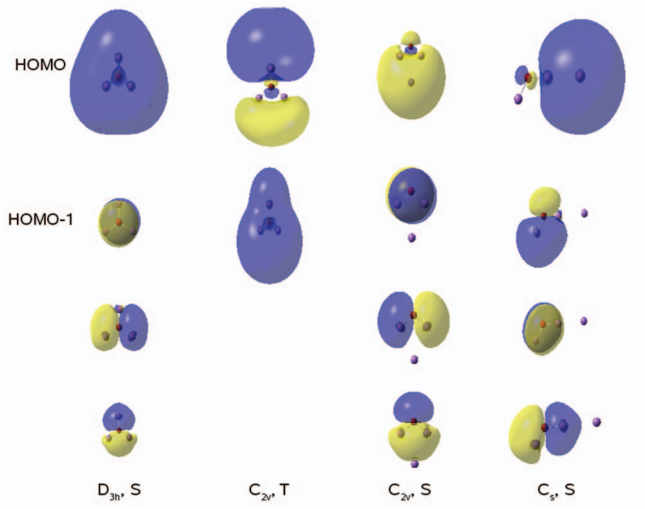

FIG. 3. Na_3O molecular orbitals for D_{3h} singlet, C_{2v} triplet, C_{2v} singlet, and C_s singlet structures (contour 0.05).

rounded by a triangle of three sodium atoms. After several failed attempts by us to attribute the observed photoelectron spectrum[17] entirely to such an anionic species, we considered different nuclear distributions inspired by our previous studies on Li_3O.[14] Similar minima, located here closer to the global minimum, were found. Whereas the C_{2v} and C_s singlet structures were about 1.5 eV higher than the global D_{3h} minimum in the Li_3O^- case, the equivalent Na_3O^- structures are only 1.0 eV over the ground state (Figs. 1 and 2). These structures are not likely to be observed at experimental temperatures. An additional structure with the oxygen atom facing a vertex of the Na_3 triangle from the exterior was found to have a triplet ground state 3.5 eV higher than the global minimum. This structure will be omitted in the following discussions.

The global minimum of the anion is characterized by a central oxygen surrounded by three sodium atoms in a D_{3h} structure with O–Na bond lengths of 2.09 Å. The latter result is about 0.3 Å longer than the Li–O distance in Li_3O^-. This is not surprising because the atomic radius of the sodium is about 0.3 Å larger than that of the lithium. In addition, the Na–O bond is expected to have more ionic character where the negative charge is more localized on the oxygen atom. The Mulliken charge distribution is $Na_3{}^{0.5}O^{-1.5}$ (Fig. 2), whereas it was approximately $Li_3{}^{0.0}O^{-1.0}$ for the hyperlithiated anion. The triplet state possesses C_{2v} symmetry, a result that is consistent with the occupation of one of the in-plane orbitals by an α electron. The metal-oxygen antibonding character of this orbital leads to a longer length for the bond lying along the C_2 axis, as shown in Fig. 3, column C_{2v} T.

The C_s and C_{2v} structures possess distinctive charge distributions in their ground states. If the negative charge is, as expected from electronegativity differences, localized on the oxygen atom in the D_{3h} structure, negative charges are shared between the oxygen and the peripheral sodium atom in the singlet C_s and C_{2v} structures (Fig. 2). One can rationalize this behavior by looking at the shapes of the pertinent molecular orbitals (Fig. 3). In particular, the highest occupied molecular orbital (HOMO) of the C_s structure is clearly centered on the peripheral sodium atom, but this orbital is shared more between the oxygen atom and the peripheral sodium in the singlet C_{2v} case. This explains the higher negative charge on the sodium in the C_s structure. Thus, the C_s charge distribution is closer to $Na_2O^0Na^{-1}$, whereas, in the singlet C_{2v} case, it is $Na_2O^{-0.7}Na^{-0.3}$.

A doublet C_{2v} structure was found in 1997[7] to be the global minimum for Na_3O according to Hartree-Fock calculations using a (14*s*3*p*/7*s*3*p*) basis set for Li and a (14*s*8*p*1*d*/7*s*4*p*1*d*) basis for O. However, in 1998, a D_{3h} ground state was found from a theoretical study that used the SVP+ basis set and DFT-BP86 methods and confirmed this conclusion with MP2/TZVPP calculations.[8] Similar contradictions in the literature preceded our study of Li_3O.[14] Here, we find that the D_{3h} structure is the global minimum using the highly correlated CCSD(T) method with the 6-311+G* basis set.

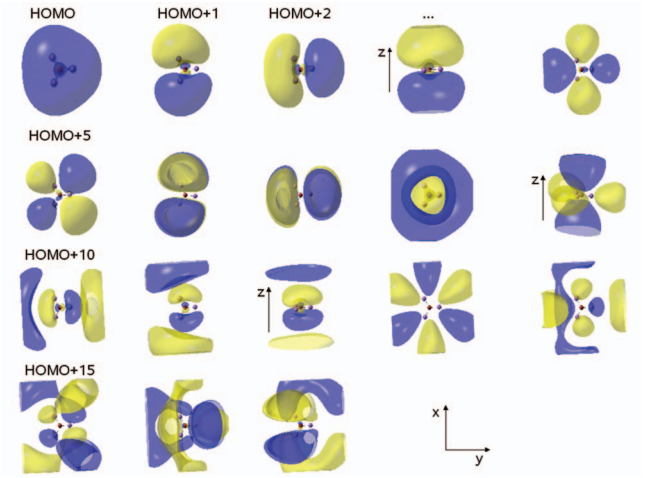

FIG. 4. Molecular orbitals involved in neutral-to-cation ionizations (D_{3h} geometry, contour, or isovalue = 0.005). The x and y axes are in the plane of the page unless the z axis is shown explicitly in the plane next to a given orbital (contour 0.05).

Electron propagator calculations

Despite the similarity between the main features of the observed Li_3O^- and Na_3O^- spectra, EPT calculations show that the initial states that correspond to the calculated peaks can be different. Table I summarizes the BD-T1 results on the VEDEs of the anionic structures.

The lowest, calculated VEDE of 0.6 eV for the D_{3h} structure can confidently be attributed to the first low intensity peak of the spectrum at 0.6–0.7 eV[17] and involves the diffuse HOMO of Na_3O^-. The HOMO-1 orbital is responsible for the far-right peak centered around 3.4 eV in the spectrum. This orbital is mainly composed of the p_z atomic orbital of the oxygen that is perpendicular to the nuclear plane. For the sake of comparison, we note that the HOMO-1 orbital of the Li_3O^- was not assigned to an experimental feature because its VEDE is higher than the photon energy, ~3.5 eV. The destabilization of this orbital in the Na_3O^- case can be related to the longer bond lengths that disfavor the very small constructive interference between the sodium and oxygen atomic orbitals.

TABLE I. BD-T1 VEDEs (eV) of singlet, ground-state structures (see Fig. 3) of Na_3O^-.

Structure	Initial state and basis sets	VEDE			
D_{3h}	$^1A'_1$	$5e'$	$5e'$	$2a_2''$	$6a_1'$
	6-311+G* +diff.[a]	3.85	3.85	3.43	0.60
	6-311+G(2df) +diff.	3.95	3.95	3.57	0.61
C_{2v}	$^1A_1$	$6b_2$	$10a_1$	$3b_1$	$11a_1$
	6-311+G* +diff.	2.31	2.30	1.97	1.23
	6-311+G(2df) +diff.	2.41	2.40	2.10	1.26
C_s	$^1A'$	$15a'$	$4a''$	$16a'$	$17a'$
	6-311+G* +diff.	2.60	2.60	2.58	1.20

[a]The definition of the extra diffuse functions can be found in the computational details section.

The following MOs (HOMO-2 and HOMO-3), centered on the p_x and p_y orbitals of the oxygen, are more stable and thus, need higher energies for electron detachment (see Table I).

If the C_s and C_{2v} singlet species were present in the experimental samples, they would be responsible for peaks at 1.2, 2.1, 2.4, and 2.6 eV, but these structures are unlikely to be observed under normal experimental conditions given their very high energy relative to that of the D_{3h} anion. However, the triplet species of the structure composed of an oxygen atom surrounded by three sodium atoms may be present in the experimental sample due to its relative stability. This structure lies 0.22 eV higher in energy than the ground state and has two singly occupied molecular orbitals that correspond to the VEDEs given in Table II. The shapes of these MOs are displayed in Fig. 3, column C_{2v}, T. The first VEDE of the triplet at 0.5 eV approximately coincides with the broad, low-intensity feature at 0.6–0.7 eV in the spectrum. The $11a_1$ orbital of the triplet seems responsible for the second experimental peak centered on 1.1 eV. This MO possesses a similar shape to that of the HOMO of the D_{3h} structure. Its relatively higher stability can be attributed to stronger bonding between the two lower sodium atoms in Fig. 3 that compensates for some of this orbital's antibonding oxygen-sodium character.

The calculated pole strengths display the reliability of the calculated transition energies via EPT. The results of Table III indicate that correlation effects are moderately strong and support use of the renormalized BD-T1 approximation. The PSs of the triplet state (see Table IV) are higher relative to those of the singlet state. These results provide justification for the use of the perturbative P3 treatment for this open-shell state.

The lowest peak corresponding to the neutral doublet state is the second peak (from right to left) on the right side of the photoelectron spectrum,[17] centered around 3 eV. Here again, as in the Li_3O case,[14] only the D_{3h} and C_{2v} structures of the anion singlet and triplet respectively will be taken into account (see Table V). The corresponding orbital is almost identical to the HOMO of the singlet anion. Of course, the removal of an electron from this orbital is energetically more demanding than in the case of the anion's VEDE because of the lack of intra-orbital electron-electron repulsion.

TABLE III. BD-T1 pole strengths for VEDEs of singlet anions.

Structure	Initial state and basis sets	Pole strength			
D_{3h}	$^1A'_1$	$5e'$	$5e'$	$2a_2''$	$6a_1'$
	6-311+G* +diff.	0.87	0.87	0.79	0.83
	6-311+G(2df) +diff.	0.87	0.87	0.79	0.83
C_{2v}	$^1A_1$	$6b_2$	$10a_1$	$3b_1$	$11a_1$
	6-311+G* +diff.	0.81	0.81	0.82	0.86
	6-311+G(2df) +diff.	0.81	0.81	0.82	0.86
C_s	$^1A'$	$15a'$	$4a''$	$16a'$	$17a'$
	6-311+G* +diff.	0.81	0.83	0.85	0.85

The low intensity peak at about 2.5 eV can be assigned to the $6e'$ MO of the D_{3h} neutral structure and $12a_1$ and $7b_2$ of the C_{2v} structure. The low intensity of this peak might be rationalized from the shapes of the corresponding molecular orbitals. Removal of an electron from the degenerate, in-plane HOMO +1, and HOMO +2 orbitals in Fig. 4 will produce a structural change. In consequence, the overlap between the vibrational normal vectors of the initial and final states is expected to be relatively small in this case. The following ionization confirms this observation, for it involves the diffuse, out-of-plane $3a_2''$ ($4b_1$ in the C_{2v} structure) orbital. In this case, the observed intensity at 1.9 eV[17] is much higher.

The $7e'$ orbitals of the D_{3h} structure together with the $13a_1$ and $8b_2$ orbitals of the C_{2v} structure are responsible for the highest peak at 1.7–1.8 eV in the observed spectrum.[17] These degenerate, d-like orbitals have nonbonding character and the removal of an electron from these levels will have only a small structural effect.

Our data may be compared to the theoretical work by Bonacic-Koutecky *et al.*[7] and the experimental-theoretical paper by Hampe *et al.*[9] on the prediction and measurement of the optical spectrum of Na_3O. The depletion spectrum in the range of 1.3–3.3 eV is provided in the latter paper. The nature of the excited states and their positions will be compared here. The first two, low intensity, peaks observed in the experimental spectrum at 1.3 and 1.4 eV correspond to the $3a_2'' \leftarrow 6a_1'$ and $7e' \leftarrow 6a_1'$ transitions, respectively. (Energy differences inferred from Table V are 1.3 and 1.4 eV, respectively). Our attribution of the peaks differs slightly from those of Hampe *et al.*, who state that their excitation energy values are overestimated. It is noteworthy that this study leads to different orders of excited

TABLE II. P3 VEDEs (eV) for the triplet state of Na_3O^-.

$^3A_1$	$11a_1$	$12a_1$
6-311+G* +diff.	1.09	0.49
6-311+G(2df) +diff.	1.10	0.50

TABLE IV. Pole strengths for VEDEs of the triplet anion.

$^3A_1$	$11a_1$	$12a_1$
6-311+G* +diff.	0.97	0.97
6-311+G(2df) +diff.	0.97	0.97

TABLE V. BD-T1 IEs (eV) of D_{3h} and C_{2v} Na_3O calculated as EAs of Na_3O^+.

	D_{3h}					C_{2v}			
	6-311+G* +diff.		6-311+G(2df) +diff.			6-311+G* +diff.		6-311+G(2df) +diff.	
	EA	PS[a]	EA	PS		EA	PS	EA	PS
$6a_1'$	3.07	0.99	3.09	0.99	$11a_1$	3.12	0.99	3.14	0.99
$6e'$	2.43	0.99	2.44	0.99	$12a_1$	2.46	0.99	2.48	0.99
$6e'$	2.43	0.99	2.44	0.99	$7b_2$	2.41	0.99	2.41	0.99
$3a_2''$	1.76	0.99	1.81	0.99	$4b_1$	1.78	0.99	1.83	0.99
$7e'$	1.64	0.99	1.67	0.99	$13a_1$	1.68	0.99	1.70	0.99
$7e'$	1.64	0.99	1.67	0.99	$8b_2$	1.60	0.99	1.62	0.99
$2e''$	1.36	0.99	1.39	0.99	$5b_1$	1.38	0.99	1.42	0.99
$2e''$	1.36	0.99	1.39	0.99	$14a_1$	1.36	0.99	1.39	0.99
$7a_1'$	1.34	0.99	1.37	0.99	$2a_2$	1.34	0.99	1.37	0.99
$8a_1'$	1.18	0.99	1.26	0.99	$15a_1$	1.18	0.99	1.26	0.99
$8e'$	1.10	0.99	1.13	0.99	$16a_1$	1.11	0.99	1.14	0.99
$8e'$	1.10	0.99	1.13	0.99	$9b_2$	1.09	0.99	1.12	0.99
$4a_2''$	0.94	0.99	0.96	0.99	$6b_1$	0.94	0.99	0.97	0.99
$2a_2'$	0.78	0.99	0.96	0.99	$10b_2$	0.80	0.99	0.96	0.99
$9e'$	0.76	0.99	0.87	0.99	$17a_1$	0.78	0.99	0.88	0.99
$9e'$	0.76	0.99	0.87	0.99	$11b_2$	0.73	0.99	0.85	0.99
$3e''$	0.67	0.99	0.78	0.99	$18a_1$	0.70	0.99	0.80	0.99
$3e''$	0.67	0.99	0.78	0.99	$7b_1$	0.66	0.99	0.78	0.99
$9a_1'$	0.59	0.99	0.78	0.99	$19a_1$	0.59	0.99	0.79	0.99

[a]PS = Pole strength.

states depending on the use of equation-of-motion, coupled-cluster singles and doubles (EOM-CCSD) or simple molecular orbital schemes (compare the order of excited states in Figs. 3 and 5 in Ref. 9). According to the authors, such results complicated the application of a qualitatively simple molecular orbital scheme to the spectra. Electron propagator methods suffer from no such conceptual impediments, for correlated transition energies are rigorously connected to their corresponding Dyson orbitals. These results may be systematically improved with higher levels of theory. The large, high intensity bands (Fig. 3(b) in Reference 9), observed between 1.5 and 1.8 eV, can be attributed to excitations from $6a_1'$ to $2e''$, $7a_1'$, and $8a_1'$. These transitions are electric-dipole-forbidden, but experience shows that exceptions to these rules, induced perhaps by vibronic effects, are not uncommon. Another feature seen near 1.9 eV may be assigned to the excitation from $6a_1'$ to $8e'$ calculated to be 1.96 eV. The large, high-energy peak in the experimental spectrum around 2.1–2.3 eV seems to be the result of a large number of excitations to closely-space orbitals such as $4a_2''$, $9e'$, $2a_2'$, and $3e''$.

Bonacic-Koutecky *et al.* found a C_{2v} ground state for Na_3O.[7] They also found a C_{2v} ground state for Li_3O, but, as we discussed in our earlier paper[14] on Li_3O and its anion, we conclude that the ground state structures for these two molecules are D_{3h}, as confirmed also by several recent papers.[3,6,9,32] Our order of the excited states obtained from BD-T1 calculations on the C_{2v} structure agrees with the one given in Reference 7 (Fig. 1 (right side)): A_1, B_2, B_1. However, irreducible representations of only the first three excited states are given in the paper and therefore we cannot compare for higher excited states. Concerning the energy levels of the excited states on the other hand, more important disagreement can be found between our results and those of Bonacic-Koutecky *et al.* One of the reasons for this may be the use of electron core potentials for the oxygen and sodium atoms. Thus, instead of 0.9, 0.9, and 1.6 eV for the first three excitations, we obtained 0.67, 0.73, and 1.31 eV.

CONCLUSIONS

The present paper presents EPT calculations of the VEDEs and IEs of Na_3O^- and Na_3O, respectively. We find geometrical minima other than the D_{3h} singlet and C_{2v} triplet states of the anionic species, but these nuclear structures are too high in energy to be included in the interpretation of the observed photoelectron spectrum. As in the previous case of the interpretation of the Li_3O^- spectrum[14,17] that we discussed recently, we find that a sequential two photon absorption mechanism could be responsible for the main features of the observed spectrum. Na_3O^- remains an interesting case, for the HOMO—1 of the D_{3h} singlet also contributes to the high-energy transitions together with the higher excited states of the neutral species.

IEs of the ground and excited states of Na_3O also have been determined, with the vertical IE of the ground state being 3.09 eV. Our calculations on the vertical IE of Li_3O yield a higher value, 3.45 eV.[14] Our data are also validated by the new experimental study of the excited states of Na_3O.

ACKNOWLEDGMENTS

This work was supported by the National Science Foundation (Grant No. CHE-0809199) to Auburn University. The

authors thank O. Dolgounitcheva and V. G. Zakrzewski for valuable discussions and technical assistance.

[1]P. V. R. Schleyer, E. U. Wuerthwein, and J. A. Pople, J. Am. Chem. Soc. **104**, 5839 (1982).
[2]G. L. Gutsev and A. I. Boldyrev, Chem. Phys. Lett. **92**, 262 (1982).
[3]A. C. Reber, S. N. Khanna, and A. W. Castleman, J. Am. Chem. Soc. **129**, 10189 (2007).
[4]P. D. Dao, K. I. Peterson, and A. W. Castleman, J. Chem. Phys. **80**, 563 (1984).
[5]D. T. Vituccio, R. F. W. Herrmann, O. Golonzka, and W. E. Ernst, J. Chem. Phys. **106**, 3865 (1997).
[6]V. G. Zakrzewski, W. von Niessen, A. I. Boldyrev, and P. von Ragué Schleyer, Chem. Phys. Lett. **197**, 195 (1992).
[7]V. Bonačić-Koutecký, J. Pittner, R. Pou-Amerigo, and M. Hartmann, Z. Phys. D: At., Mol. Clusters **40**, 445 (1997).
[8]S. D. Elliott and R. Ahlrichs, J. Chem. Phys. **109**, 4267 (1998).
[9]O. Hampe, G. M. Koretsky, M. Gegenheimer, C. Huber, M. M. Kappes, and J. Gauss, J. Chem. Phys. **107**, 7085 (1997).
[10]E. Clementi, J. Chem. Phys. **47**, 1865 (1967).
[11]P. M. Guyon and J. Berkowitz, J. Chem. Phys. **54**, 1814 (1971).
[12]E. U. Wuerthwein and P. V. R. Schleyer, J. Am. Chem. Soc. **106**, 6973 (1984).
[13]E. Rehm, A. I. Boldyrev, and P. V. R. Schleyer, Inorg. Chem. **31**, 4834 (1992).
[14]S. Zein and J. V. Ortiz, J. Chem. Phys. **135**, 164307 (2011).
[15]C. H. Wu, H. Kudo, and H. R. Ihle, J. Chem. Phys. **70**, 1815 (1979).
[16]P. Lievens, P. Thoen, S. Bouckaert, W. Bouwen, F. Vanhoutte, H. Weidele, R. E. Silverans, A. Navarro-Vázquez, and P. V. R. Schleyer, J. Chem. Phys. **110**, 10316 (1999).
[17]D. Wang, J. D. Graham, A. M. Buytendyk, and K. H. Bowen, J. Chem. Phys. **135**, 164308 (2011).
[18]J. V. Ortiz, J. Chem. Phys. **104**, 7599 (1996).
[19]J. V. Ortiz, Int. J. Quant. Chem. **75**, 615 (1999).
[20]J. V. Ortiz, Chem. Phys. Lett. **296**, 494 (1998).
[21]M. S. Deleuze and S. Knippenberg, J. Chem. Phys. **125**, 104309 (2006).
[22]E. Weigold and I. E. McCarthy, *Electron Momentum Spectroscopy* (Kluwer, New York, 1999).
[23]J. Itatani, J. Levesque, D. Zeidler, H. Niikura, H. Pepin, J. C. Kieffer, P. B. Corkum, and D. M. Villeneuve, Nature **432**, 867 (2004).
[24]S. Patchkovskii, Z. Zhao, T. Brabec, and D. M. Villeneuve, Phys. Rev. Lett. **97**, 123003 (2006).
[25]M. Yamazaki, T. Horio, N. Kishimoto, and K. Ohno, Phys. Rev. A **75**, 032721 (2007).
[26]R. Flores-Moreno, J. Melin, O. Dolgounitcheva, V. G. Zakrzewski, and J. V. Ortiz, Int. J. Quant. Chem. **110**, 706 (2010).
[27]M. J. Frisch, G. W. Trucks, H. B. Schlegel *et al.*, GAUSSIAN 03, Revision B.04, Gaussian, Inc., Wallingford, CT, 2003.
[28]R. J. Bartlett, J. Phys. Chem. **93**, 1697 (1989).
[29]K. Raghavachari, G. W. Trucks, J. A. Pople, and M. Head-Gordon, Chem. Phys. Lett. **157**, 479 (1989).
[30]R. Krishnan, J. S. Binkley, R. Seeger, and J. A. Pople, J. Chem. Phys. **72**, 650 (1980).
[31]M. J. Frisch, J. A. Pople, and J. S. Binkley, J. Chem. Phys. **80**, 3265 (1984).
[32]M. Gutowski and J. Simons, J. Phys. Chem. **98**, 8326 (1994).